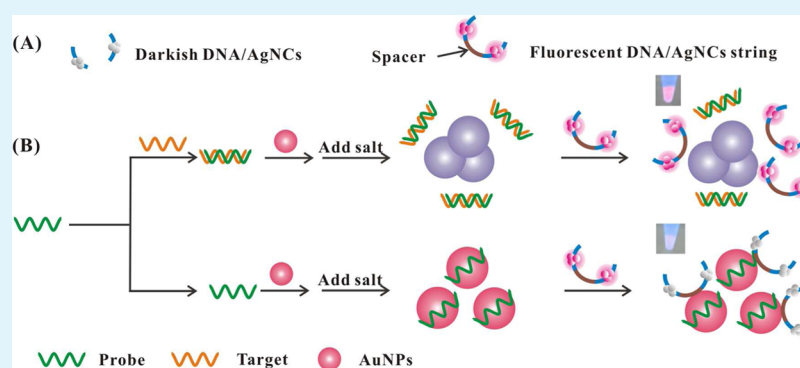# Label-Free Detection of Sequence-Specific DNA Based on Fluorescent Silver Nanoclusters-Assisted Surface Plasmon-Enhanced Energy Transfer

Jin-Liang Ma,[†] Bin-Cheng Yin,*[,†] Huynh-Nhu Le,[†] and Bang-Ce Ye*[,†,‡]

[†]Lab of Biosystem and Microanalysis, Biomedical Nanotechnology Center, State Key Laboratory of Bioreactor Engineering, East China University of Science & Technology, Shanghai 200237, China

[‡]School of Chemistry and Chemical Engineering, Shihezi University, Xinjiang, 832000, China

Ⓢ *Supporting Information*

ABSTRACT: We have developed a label-free method for sequence-specific DNA detection based on surface plasmon enhanced energy transfer (SPEET) process between fluorescent DNA/AgNC string and gold nanoparticles (AuNPs). DNA/AgNC string, prepared by a single-stranded DNA template encoded two emitter-nucleation sequences at its termini and an oligo spacer in the middle, was rationally designed to produce bright fluorescence emission. The proposed method takes advantage of two strategies. The first one is the difference in binding properties of single-stranded DNA (ssDNA) and double-stranded DNA (dsDNA) toward AuNPs. The second one is SPEET process between fluorescent DNA/AgNC string and AuNPs, in which fluorescent DNA/AgNC string can be spontaneously adsorbed onto the surface of AuNPs and correspondingly AuNPs serve as "nanoquencher" to quench the fluorescence of DNA/AgNC string. In the presence of target DNA, the sensing probe hybridized with target DNA to form duplex DNA, leading to a salt-induced AuNP aggregation and subsequently weakened SPEET process between fluorescent DNA/AgNC string and AuNPs. A red-to-blue color change of AuNPs and a concomitant fluorescence increase were clearly observed in the sensing system, which had a concentration dependent manner with specific DNA. The proposed method achieved a detection limit of ∼2.5 nM, offering the following merits of simple design, convenient operation, and low experimental cost because of no chemical modification, organic dye, enzymatic reaction, or separation procedure involved.

KEYWORDS: *DNA detection, surface plasmon enhanced energy transfer, fluorescent silver nanoclusters, gold nanoparticle, fluorescence enhancement*

■ INTRODUCTION

Over the past decades, noble nanoscale metals have attracted considerable scientific interests in a variety of application areas, including sensing, biomedicine, and optics.[1−3] According to the different size, noble nanoscale metals can be roughly divided into three categories: bulk nanoparticles, small nanoparticles, and nanoclusters. In contrast to the bulk and small noble metal nanoparticles (NMNPs), noble metal nanoclusters (NMNCs) (e.g., Ag, Au, and Pt) consist of several to even one hundred with the size comparable to the Fermi wavelength of conduction electrons, offering the missing link between metal atoms and nanoparticles.[4] In this size regime, metal nano-

clusters have possessed dramatically different optical, electronic, and chemical properties as compared to those of much larger nanoparticles because of the electronic transitions between molecule-like energy levels.[5,6] Significantly, these nanoclusters have displayed intense size-dependent fluorescent emission upon photoexcitation in the UV−visible range.

Among these molecule-scale nanoclusters, silver nanoclusters (AgNCs) have been widely exploited because of their attractive

Table 1. Sequence Information for DNA Oligonucleotides Used in This Study

name	Sequence[a] (5'-3')
DNA1	CCCTTAATCCCC
DNA2	CCCTAACTCCCC
DNA3	CCCTTAATCCCCTTTTTCCCTAACTCCCC
DNA4	CCCTTAATCCCCTTTTTTTTTTTTTTTCCCTAACTCCCC
DNA5	CCCTTAATCCCCTTTTTTTTTTTTTTTTTTTTTTTCCCTAACTCCCC
DNA6	CCCTTAATCCCCGTTGACTTGTGTTGCCCTAACTCCCC
DNA7	CCCTTAATCCCCCAACACAAGTCAACGCCCTAACTCCCC
DNA8	CCCTTAATCCCCCTATACAACCTACTACCCTAACTCCCC
DNA9	CCCTTAATCCCCTTATATAATTTATTACCCTAACTCCCC
S–PEG5	CCCTTAATCCCCTT-CH2–(CH2–O–CH2)5–CH2–TTCCCTAACTCCCC
S–C3	CCCTTAATCCCCTT-CH2–CH2–CH2–TTCCCTAACTCCCC
probe	AACTATACAACCTACTACCTCA
T1	TGAGGTAGTAGGTTGTATAGTT
T2	TGAGGTAGGAGGTTGTATAGTT
T3	AGAGGTAGTAGGTTGCATAGTT
T4	TAACACTGTCTGGTAAAGATGG

[a]The bases in blue color represent the AgNC-nucleation sequences used as templates to synthesize DNA/AgNCs. The bases in brown color represent oligo spacer between two AgNC emitters. The bases in red color represent the mutation sites in the tested DNAs compared with target T1.

features of excellent brightness and high fluorescence quantum yield, tunable fluorescence emission, and good photostability.[7] In particular, water-soluble DNA-scaffolded AgNCs (DNA/AgNCs), first reported by Braun and co-workers in 1998,[8] are highly fluorescent, more photostable, and cost-effective to synthesize, and have found a wide applications in cellular imaging, biological labeling, and chemical/biological sensing in recent years.[9−13] It has proven that the fluorescence emission property of DNA/AgNCs is sensitive to the DNA template in its base, base sequence, and length, and can be dramatically altered ranging from visible to near-IR under change in either emitter or its nearby sequence.[14−16] Usually, DNA/AgNCs have been employed as fluorophores directly to detect various analytes, such as metal ions,[17,18] ochratoxin A,[19] micro-RNAs,[20−23] cancer cells,[24] and proteins,[25] and to develop logic devices.[26] Differently, Yeh and co-workers reported an interesting phenomenon that dark DNA/AgNCs could be transformed into bright red-emitting clusters with ∼500-fold fluorescence enhancement when placed in proximity to guanine-rich (G-rich) overhang.[27] On the basis of the superiority of ultrahigh signal-to-background ratio, a few fluorescence turn-on designs have been developed by manipulating the distance between the DNA/AgNCs and G-rich DNA.[28−32] Enlightened by the fluorescence light-up phenomenon of DNA/AgNCs via hybridization upon G-rich DNA activator, we recently reported a new mode to light up adjacent, dark DNA/AgNC probes.[33] We found that there was a stronger fluorescence enhancement up to ∼1500-fold when two dark DNA/AgNCs were placed together to form a probe pair through their complementary sequences. Based on this finding, we wonder whether there is fluorescence enhancement when two dark AgNCs are simultaneously scaffolded with the same DNA template, located at each end of the DNA template. It was observed that the silver nanoclusters (named DNA/AgNC string) also displayed a bright fluorescence emission, which provides a new form of fluorescent AgNCs.

Gold nanoparticles (AuNPs) are well-known for their ultrahigh fluorescence quenching capability upon the organic dyes. In 2001, Dubertret and co-workers first designed an AuNP-based molecular beacon by employing a stem-loop structure tagged with a fluorophore and 1.4 nm diameter AuNP as a quencher.[34] After that, AuNPs functionalized with dye-labeled DNAs have been extensively utilized to develop fluorescent biosensors via the strong adsorption between AuNPs and fluorescent dyes.[35−38] It has been reported that specific surface plasmon resonance (SPR) characteristics

supported by NMNPs triggered strong fluorescence quenching behavior via surface plasmon-enhanced energy transfer (SPEET) between NMNCs and NMNPs, such as gold nanocluster (AuNCs) and AuNPs or silver nanoparticles (AgNPs).[39,40] Similar to Förster resonance energy transfer (FRET) via dipole−dipole interaction of molecular donor and acceptor, SPEET belongs to the dipole−surface interaction between the molecular metal nanocluster and nanoparticle due to large surface-to-volume ratio in nanometal surface.[41] In this work, we have combined the fluorescent DNA/AgNC string and ultrahigh fluorescence quenching capability of AuNPs to develop a rapid, label-free method for specific DNA detection via the mechanism of SPEET process. The SPEET process takes place as followed, the proposed fluorescent DNA/AgNC string electrostatically binds onto the surface of unmodified AuNP colloid, and correspondingly AuNPs serve as "nano-quencher" to quench the fluorescence of DNA/AgNC string. It is well-known that flexible ssDNA is easily adsorbed onto unmodified AuNP colloid and prevents salt-induced AuNP aggregation because of strong interparticle electrostatic repulsion between ssDNA-adsorbed AuNPs, whereas stiffer dsDNA with exposed negatively charged phosphate backbone has weak adsorption onto the negatively charged AuNPs and cannot efficiently prevent salt-induced AuNP aggregation. Taking advantage of the different binding properties of ssDNA and dsDNA toward AuNPs, the presence of target DNA would induce the aggregation of AuNP colloid under high ionic strength condition because of the formation of dsDNA with single-stranded probe in our detection system. The resultant AuNP aggregation makes DNA/AgNC string's binding negligible, leading to a weakened SPEET process and a remarkable fluorescence signal. Based on this working principle, we have designed a novel, label-free DNA detection method by coupling DNA/AgNC string and colloidal AuNPs, which eliminates the requirement for chemical modification, organic dye, enzymatic reaction, or separation procedure.

■ EXPERIMENTAL SECTION

Reagents and Materials. Oligonucleotides used were custom-synthesized by Sangon Biological Engineering Technology & Services Co., Ltd. (Shanghai, China). The sequences of these oligonucleotides are listed in Table 1. Hydrogen tetrachloroaurate (III) dehydrate (HAuCl4) and silver nitrate (AgNO3) were purchased from Sinopharm Chemical Reagent Co., Ltd. (Shanghai, China). Sodium borohydride (NaBH4) was purchased from Tianlian Fine Chemical Co., Ltd. (Shanghai, China). All chemicals used were of analytical reagent, obtained from commercial sources, and directly used without

Scheme 1. (A) Pictorial Representation of Fluorescent DNA/AgNC String Containing Two Dark DNA/AgNCs at the Termini and Oligo Spacer in the Middle; (B) Pictorial Representation of the Proposed Label-Free Method for Specific DNA Detection Based on SPEET Process between Fluorescent DNA/AgNC String and AuNP Colloid
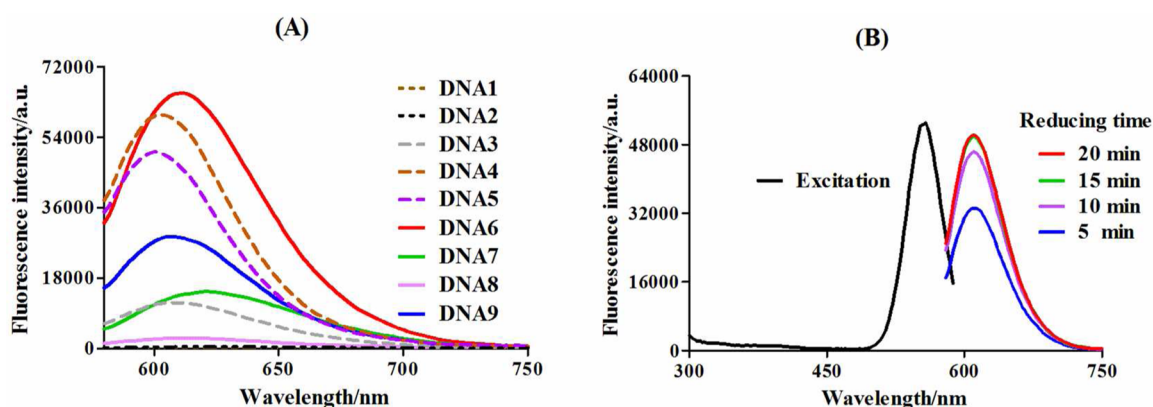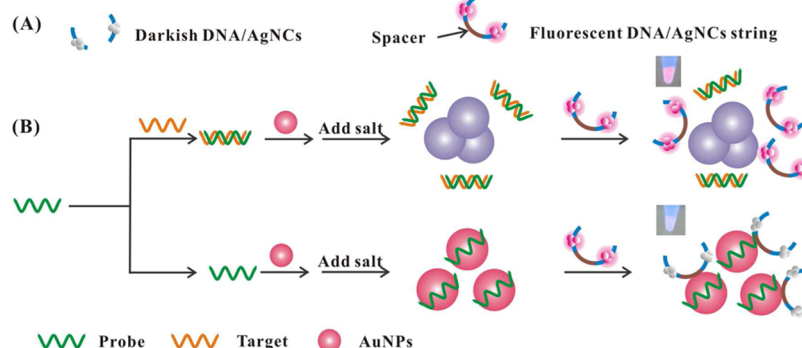
Figure 1. (A) Fluorescence emission spectra responses of AgNCs scaffolded by different DNA templates. (B) Time-dependent measurements of fluorescence emission and excitation spectra of the DNA6/AgNC string. Fluorescence emission spectra were recorded at 5, 10, 15, and 20 min after mixing DNA6 with $AgNO_3$ and $NaBH_4$, respectively. Ex: 560 nm. The excitation spectrum was recorded at 15 min after mixing the DNA6 with $AgNO_3$ and $NaBH_4$. Em: 608 nm.

additional purification. The solutions were prepared using distilled water purified by a Milli-Q water purification system (Millipore Corp., Bedford, MA, USA) with an electrical resistance of 18.2 MΩ cm.

Instrumentation. UV−vis absorption and fluorescence spectra were measured by a fluorescence microplate reader (Bio-Tek Instrument, Winooski, USA) using transparent 96-well microplate and black 96-well microplate (Corning Inc., NY, USA), respectively. Transmission electron microscope (TEM) measurement was performed on Jeol JEM-2100 instrument (JEOL Ltd., Japan).

Preparation Procedures for AuNP Colloid and Fluorescent DNA/AgNC String. The colloidal solution of citrate-AuNPs in 13 nm diameter with a concentration of 3.1 nM was prepared according to the reported method.[42] Fluorescent DNA/AgNC string was prepared in a molar ratio DNA/Ag$^+$/NaBH$_4$ of 1:6:6 according to the reported literature with minor modification.[43] Briefly, fluorescent DNA/AgNC string was prepared by adding an aliquot of $AgNO_3$ solution (1 mM, 2.4 μL) to DNA template solution (20 μM, 20 μL) with a Ag$^+$-to-DNA molar ratio of 6:1 in a phosphate buffer (1.9 mM NaH_2PO_4, 3.1 mM Na_2HPO_4, 50 mM $NaNO_3$, pH 7.0) in a total volume of 200 μL. Then, the mixture was incubated in the dark at room temperature for 20 min. Subsequently, an aliquot of fresh $NaBH_4$ solution (1 mM, 2.4 μL) was added to the above mixture followed by vigorous shaking for 5 s, and finally the resultant mixture was kept in the dark at room temperature for 15 min before use.

Specific DNA Detection Procedure. The typical experiment for specific DNA detection involved three steps. First, a series of T1 aliquots at different concentrations were added to the probe solution (10 μM) in phosphate buffer solution (3.8 mM NaH_2PO_4, 6.2 mM Na_2HPO_4, 300 mM $NaNO_3$, pH 7.0), respectively, and incubated for 5 min at room temperature. Second, the above probe and T1 solution

was mixed with 40 μL AuNP colloidal solution (6.2 nM) and 50 μL phosphate buffer solution (3.8 mM NaH_2PO_4, 6.2 mM Na_2HPO_4, 300 mM $NaNO_3$, pH 7.0) with a total reaction volume of 100 μL. After that, 100 μL fluorescent DNA/AgNC string was added, and then the resultant mixture was kept in the dark at room temperature for 5 min. Third, the resultant mixture was transferred to a black 96-well microplate and scanned by the fluorescence microplate reader from 580 and 750 nm under an excitation at 560 nm. Unless noted otherwise, all experiments in this work were repeated three times.

Detection of Specific DNA in Serum Sample. Serum obtained were loaded into centrifugal filtration devices (Molecular weight cutoff or MWCO 50 kDa, Millipore Amico Ultra), centrifuged at 6000 rpm for 20 min.[31] Then, specific DNA targets with different concentrations were spiked into pretreated serum.

■ RESULTS AND DISCUSSION

The working principle of the proposed method for label-free DNA detection based on SPEET process between fluorescent DNA/AgNC string and unmodified AuNP colloid is illustrated in Scheme 1. The proposed fluorescent DNA/AgNC string is designed by linking two dark AgNCs as shown in Scheme 1A. Two reported AgNC-nucleation sequences are chosen to produce dark DNA/AgNCs under the excitation of 560 nm. A rationally designed oligo spacer is employed to connect these two AgNC-nucleation sequences, and this intact DNA sequence is served as a scaffold to form fluorescent DNA/AgNC string following the Dickson's method with a slight modification.[43] As shown in Scheme 1B, the proposed
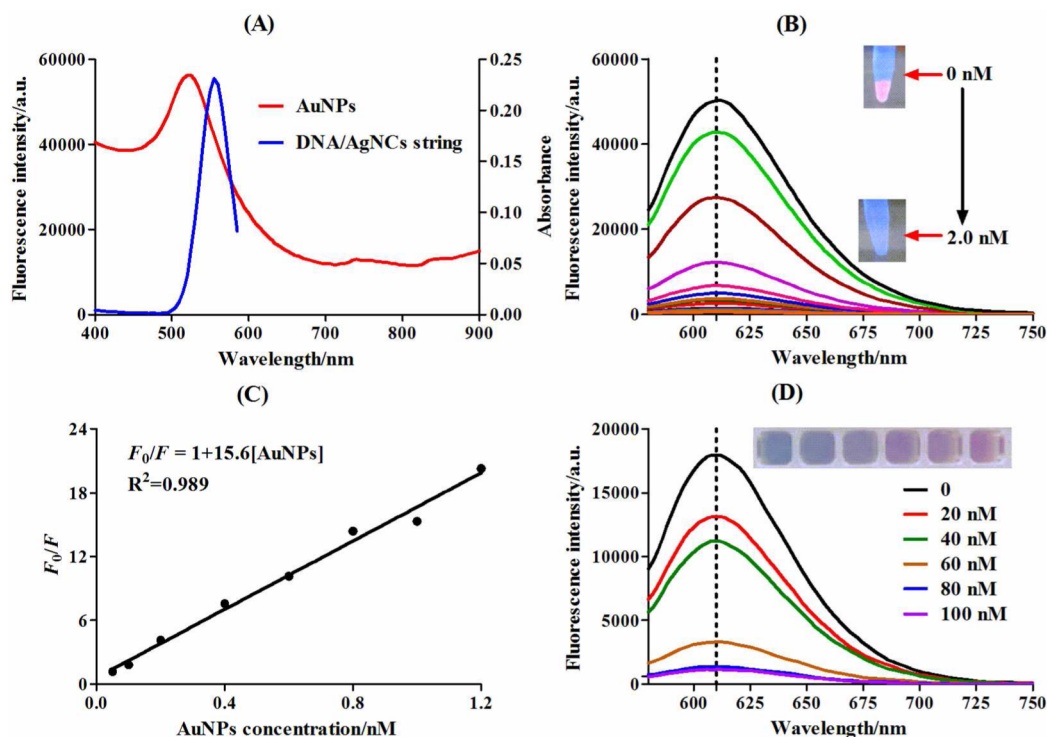
Figure 2. Investigation on SPEET process between fluorescent DNA/AgNC string and AuNP colloid. (A) Excitation spectra of the pure as-prepared DNA/AgNC string (blue line) and UV−vis spectra of AuNP colloid (red line). (B) Fluorescence emission spectra of DNA/AgNC string in phosphate buffer (0.95 mM NaH$_2$PO$_4$, 1.55 mM Na$_2$HPO$_4$, 25 mM NaNO$_3$, pH 7.0) after adding 100 μL colloidal AuNP solution at different final concentrations (0, 0.05, 0.1, 0.2, 0.4, 0.6, 0.8, 1.0, 1.2, 1.4, 1.6, 1.8, and 2.0 nM). Inset: Photograph of DNA/AgNC string solution under UV irradiation before and after adding 2.0 nM AuNP from upper to bottom, respectively. (C) Stern−Volmer plot of the data presented in B from 0.05 to 1.2 nM. (D) Fluorescence emission spectra of DNA/AgNC string after adding 100 μL mixture containing AuNP colloid (1.24 nM) and probe with increased concentrations (0, 20, 40, 60, 80, and 100 nM) in phosphate buffer solution (1.9 mM NaH$_2$PO$_4$, 3.1 mM Na$_2$HPO$_4$, 100 mM NaNO$_3$, pH 7.0). Inset: Photograph showing colorimetric responses of the mixtures containing DNA/AgNC string, AuNP colloid (1.24 nM) and probe at increased concentrations from 0 to 100 nM. From left to right are 0, 20, 40, 60, 80, and 100 nM probe.

detection system, containing a single-stranded probe complementary to target DNA, is mixed with reaction buffer or target DNA tested solution, and subsequently an AuNP solution is added. After incubation for a short time, a salt buffer with high concentration and fluorescent DNA/AgNC string solution is sequentially introduced. Then, the resultant mixture is detected by either fluorescence measurement or UV−vis characterization. In the absence of target, the single-stranded probe spontaneously adsorbs onto the surface of AuNPs to protect AuNPs from aggregation under high ionic strength condition. Similarly, subsequently added fluorescent DNA/AgNC string also spontaneously attaches onto AuNPs, leading to the fluorescence of DNA/AgNC string quenched. However, in the presence of target DNA, the single-stranded probe hybridizes with target DNA to form double-helix dsDNA, which could not prevent the salt-induced AuNP aggregation. As a result, the color of the solution changes from red to blue after the addition of salt. Afterward, the added fluorescent DNA/AgNC string stably exists without binding onto the surface of aggregated AuNPs. No SPEET process takes place. Therefore, via the efficient SPEET process, fluorescence intensity and color change in the sensing system are directly proportional to the amount of target DNA present in the tested samples.

We first performed a series of control experiments to optimize the DNA template to produce strongly emissive DNA/AgNC string. Two reported 12-nt AgNC-nucleation sequences[44] producing a yellow emitter (DNA-Y: 5′-CCCTTAATCCCC-3′, an emission maximum at 572 nm)

and a near-IR emitter (DNA-NIR: 5′-CCCTAACTCCCC-3′, an emission maximum at 705 nm) were chosen as the scaffolds for synthesis of dark AgNCs. It can be seen that the resultant AgNCs scaffolded by these two sequences both displayed very weak fluorescence emissions upon the excitation at 560 nm (DNA1, DNA2 in Figure 1A). In order to rapidly determine the proper length of spacer between two dark-AgNC-nucleation sequences, we employed poly(deoxythymidine, dT) with different lengths as models to test the fluorescence intensity of DNA/AgNC strings. Of the four bases (adenine, thymine, guanine, and cytosine), thymine exhibited the weakest affinity for silver nanocluster,[45] making this base optimal for initial screening of spacer sequence. Three DNA templates (DNA3, DNA4, and DNA5) with poly(dT) spacers of various lengths (5, 15, and 25 nt) were selected for producing emissive DNA/AgNC string, respectively. Figure 1A compares the fluorescence spectra of the tested DNA template-scaffolded AgNC strings. The highest fluorescence intensity was clearly observed for employment of DNA4 with 15-nt poly(dT) spacer (brown dash line) as a scaffold. At present, we cannot fully interpret the physical mechanism driving the fluorescence enhancement of the adjacent dark emitters and the effect of oligo spacer length on fluorescence enhancement. We preliminarily presume it is due to the distance-dependent energy and charge transfer property of the adjacent dark AgNCs,[46,47] in which too close or too far away might not favor the formation of bright DNA/AgNC string. The highly fluorescent AgNCs hosted by the DNA templates (S-PEG$_5$ and S-C$_3$) with hydrophobic spacer
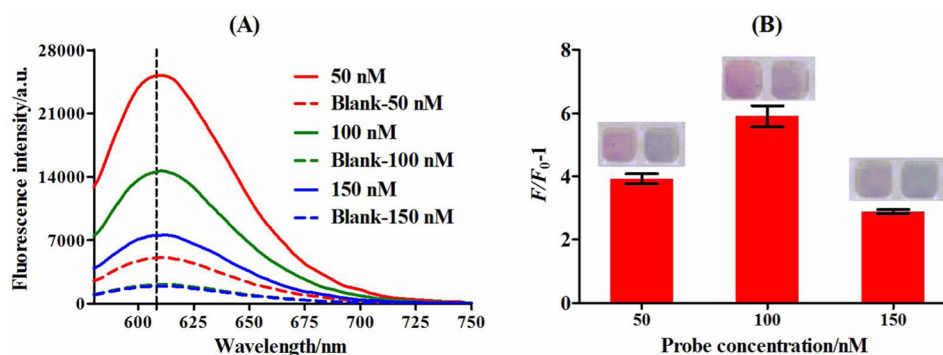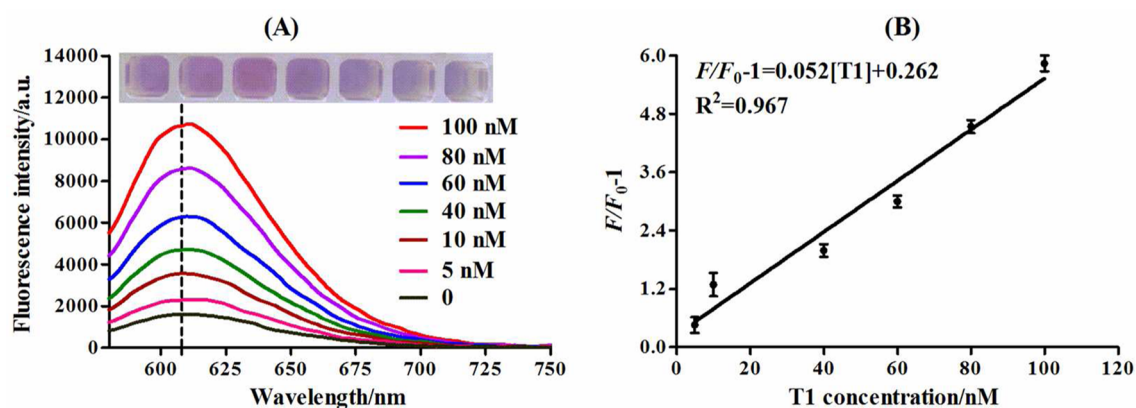
Figure 3. Investigation of probe concentration on the performance of the proposed method. (A) Fluorescence emission spectra responses to probe at different concentrations (50, 100, and 150 nM) in the absence (dash lines) and the presence (solid lines) of target T1, respectively. The concentration of target T1 was selected at the same concentration as probe (50, 100, and 150 nM). (B) Bar representing fluorescence ratio ($F/F_0 - 1$) responses in the presence of probe at different concentrations as shown in data (A), where F and F_0 are the fluorescence intensities at a peak value of 608 nm in the presence and absence of target T1, respectively. Inset: the left and right photographs represent in the absence and presence of target T1, respectively.

(PEG and hydrocarbon chain, respectively) between two emitters also supported the significance of the spacer with weaker capability of binding silver ions (Figure S1 in the Supporting Information). To further optimize the DNA template, we rationally designed four DNA templates including DNA6, DNA7, DNA8, and DNA9 with different base sequences in 15-nt oligo spacer. Upon comparison among these four DNA templates creating AgNC strings, we notice that DNA6 as a scaffold produced the highest fluorescence (red line). When irradiated for 60 min, the fluorescence intensity of DNA6/AgNCs decreases by 84.0% (Figure S2 in the Supporting Information). The quantum yield (QY) of as-prepared DNA6/AgNCs was ∼36.9% that is highest value at pH 7 and 50 mM NaNO₃ using Rhodamine B in ethanol as the reference standard (Figure S3 in the Supporting Information), whereas the QY of DNA4/AgNCs and DNA5/AgNCs are ∼16.3 and ∼2.7%, respectively. In addition, the produced DNA6/AgNC strings also showed a stronger capability to create brighter silver nanoclusters, compared to G-rich overhang-activated fluorescent AgNCs reported in Yeh's work[27] (Figure S4 in the Supporting Information). On the basis of the above results, we found that the acquirement of a class of excellent AgNCs can be enabled by not only base arrangement but also its appropriate length of spacer between two sequences producing dark emitters, which is consistent with the previous findings that DNA/AgNC formation depended greatly on the specific secondary structures of the DNA scaffolds.[48] In further work, we would devote our ongoing effort on elucidating the underlying mechanism about two issues, why double 12-nt dark clusters-nucleation sequence in the same strand can enhance the fluorescence intensity, and how the amount and arrangement of bases in spacer sequence affect the fluorescence intensity of emissive DNA/AgNC string.

Figure 1B shows the time-dependent measurements of the formation of DNA6/AgNC string recorded at various times under the excitation of 560 nm. The observation clearly demonstrates that the formation of fluorescent DNA6/AgNC string achieved the maximum emission within ∼15 min, which is faster than the reported protocols of chemical reduction of Ag nanoclusters took more than 1 h.[43] However, the reason for the faster speed of DNA/AgNC string formation is not fully understood. We assume it is likely that the structure of the DNA template containing a 15-nt oligo spacer to connect the

two dark emitters would greatly influence the conformation of DNA/AgNC string, resulting in the formation of a self-dimer or a hairpin structure to stabilize the AgNCs.[48] An excitation spectrum of DNA6/AgNC string is also given in Figure 1B by monitoring the emission at 608 nm (black line). DNA6/AgNC and DNA4/AgNC strings were characterized by TEM, as shown in Figure S5 in the Supporting Information. Because of the brighter fluorescence, DNA6 was chosen as the scaffold for preparation of fluorescent AgNC string in the subsequent experiments.

Next, we explored the SPEET process between the proposed fluorescent DNA/AgNC string and AuNP colloid. It has been demonstrated that the large overlap of the excitation spectra and AuNP absorption spectra was indispensable for SPEET.[40] As shown in Figure 2A, there was a large spectral overlap from 520 to 555 nm between the excitation spectra of emissive DNA/AgNC string (maximum excitation at 555 nm) and absorption spectra of AuNP colloid (maximum absorption at 520 nm), implying the possibility of employing emissive DNA/AgNC string as energy donor to AuNP acceptor in SPEET process, which is consistent with the quenching of AuNCs via SPEET between AuNCs and AgNPs or AuNPs.[39,40] When DNA/AgNC string was mixed with AuNP colloid at increased concentrations from 0 to 2 nM, it can be seen that the fluorescence intensity of DNA/AgNC string significantly decreased to minimum value (Figure 2B) with the quenching efficiency up to ∼99.0%, in which the quenching effect by AuNPs was also verified by excluding the disturbance of solvent except AuNPs (Figure S6 in the Supporting Information). The Stern−Volmer equation was employed to describe the concentration-dependence of the quenching effect (F_0/F) of the nanoquencher AuNPs on the fluorescence emission of DNA/AgNC string (where F_0 and F are the fluorescence intensity of AgNCs at 608 nm in the absence and presence of AuNPs, respectively). Figure 2C outlines the linear Stern−Volmer plot, the correlation equation is $F_0/F = 1 + 15.6[\text{AuNPs}]$ with a correlation coefficient R^2 of 0.989. To further investigate the correlation of fluorescence intensity of DNA/AgNC string on the existence form of AuNPs, we obtained AuNP aggregation by controlling the probe concentration after adding 10 mM phosphate buffer containing 150 mM NaNO₃, according to the previous method in which 152.3 mM NaCl was used in the reaction system with 35.3/1 of

Figure 4. Sensitivity investigation of the proposed method for specific detection of target T1. (A) Fluorescence emission spectra response in the presence of T1 at increased concentrations (0, 5, 10, 40, 60, 80, 100 nM). Ex: 560 nm. Inset: Photograph showing colorimetric responses of the detection system in the presence of various concentrations of target T1. From left to right are 0, 5, 10, 40, 60, 80, and 100 nM target T1. (B) Plot of the linear relationship between the fluorescence ratio $(F/F_0 - 1)$ and the concentration of target T1, where F and F_0 are the fluorescence intensities at a peak value of 608 nm in the presence and absence of target T1, respectively.
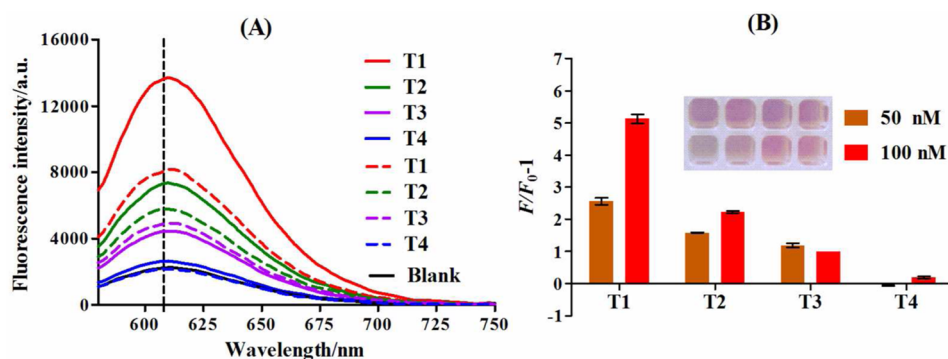
Figure 5. Selectivity investigation of the proposed method using different target DNAs. (A) Fluorescence emission spectra responses in the presence of different targets. The solid and dashed lines represent fluorescence spectra in the presence of the 100 nM and 50 nM target DNA, respectively. Ex: 560 nm. (B) The fluorescence ratio $(F/F_0 - 1)$ values obtained based on data from A, where F and F_0 are the fluorescence intensities at a peak value of 608 nm in the presence and absence of tested target, respectively. Inset: Photograph showing colorimetric responses of the detection system with different target DNAs at two tested concentrations. From left to right are T1, T2, T3, and T4.

probe/AuNPs.[49] Figure S7A, B in the Supporting Information shows the highest fluorescence of DNA/AgNCs was obtained in the phosphate buffer solution (1.9 mM NaH_2PO_4, 3.1 mM Na_2HPO_4, 50 mM $NaNO_3$, pH 7.0) and their tolerance of salt concentration was up to 100 mM, respectively. The changeless absorption spectra of Au NPs at various concentrations in the absence and presence of DNA/AgNC string removed the interference effect of DNA/AgNC-induced AuNP aggregation (Figure S8 in the Supporting Information). As shown in Figure 2D, a low level of AuNP aggregation, produced by adding great amounts of probe to AuNP colloid, would lead to a significant quenching in the fluorescence intensity. Obviously, the loss of monodisperse AuNPs would weaken SPEET process, which demonstrates that SPEET process originates from the interaction of DNA/AgNC string and AuNPs, which are in close proximity. Figure S5C in the Supporting Information exhibits characteristics of AuNP colloid by TEM.

A good signal-to-background ratio is more favorable to obtain a higher sensitivity in the detection method. The fluorescence ratio value $(F/F_0 - 1)$ was employed to calculate the signal-to-background ratio upon the addition of target DNA in the detection system, where F and F_0 are the fluorescence intensities at a peak value of 608 nm in the presence and absence of target T1, respectively. As shown in Figure 2D, the

amount of single-stranded probe directly affected the background signal of the proposed method because salt-induced AuNP aggregation was enhanced by the decrease of probe concentration, resulting in weaker SPEET process. Therefore, the concentration of probe is an important experimental factor to affect the background signal in our detection system. Three concentrations of 50, 100, and 150 nM probe were selected. Figure 3A clearly describes the fluorescence emission spectra with different probe concentrations in the absence and the presence of target T1. It can be seen that the fluorescence signal was significantly decreased with probe concentration increased. As shown in Figure 3B, 100 nM probe achieved the best signal-to-background value $(F/F_0 - 1)$. Thus, we chose 100 nM probe for the subsequent experiments.

Under the above optimized experimental conditions and according to the experimental protocol described in the Experimental Section, the sensitivity of the proposed method was carefully investigated. The fluorescence spectra of the sensing system were recorded upon the addition of target T1 at different amounts (Figure 4A). As expected, fluorescence intensity gradually increased with an increase in the concentration of target T1 from 0 to 100 nM, indicating that SPEET process proceeded in a dose-dependent manner with respect to target T1. As the probe concentration decreased

upon the hybridization with target T1 at increased concentration, the salt-induced AuNP aggregation would be at an increased level. Correspondingly, the color of the AuNPs was changed from red to blue with the increasing amount of added target T1 (Figure 4A, inset). Figure 4B shows the fluorescence change ratio ($F/F_0 - 1$) as a function of target T1 concentration (5, 10, 40, 60, 80, and 100 nM). The linear regression equation was $F/F_0 - 1 = 0.052[T1] + 0.262$ with a correlation coefficient R^2 of 0.967. The detection limit was estimated to be ~2.5 nM ($3\sigma/S$, σ is the standard deviation of the blank solution) and ~10 fold higher than the biosensor based on AgNCs only.[50] To investigate the application in biological samples, we carried out the spike-in experiment by adding target T1 with known concentrations into the pretreated serum. As shown in Table S1 in the Supporting Information, quantitative detection of specific T1 by the proposed method was achieved with an acceptable recovery and good stability. These results indicate that our proposed assay based on SPEET between DNA/AgNC string and AuNPs has a potential to apply in biological samples.

To validate the sequence specificity of the proposed method, we prepared several different target DNAs including perfect-matched, and mismatched targets (T1, T2, T3, and T4). Figure 5 exhibits the comparison of fluorescence responses toward the different targets at two concentrations of 50 and 100 nM. It is observed that the fluorescence ratio value generated by perfect-matched target T1 was the highest among other tested targets, which enables the significant discrimination between perfect-matched and single-base mismatched targets at the same concentration level. Photograph of colorimetric response of AuNP colloid also supports the sequence specificity of the proposed method. A mixture of target T1 with various fractions and T4 as interfering species was further tested. Figure S9 in the Supporting Information shows clearly that as little as 30% target DNA was easily detected, which is consistent with the previous studies.[49]

CONCLUSION

In summary, we have obtained a template forming highly fluorescent DNA/AgNC string with faster synthesis speed of 15 min. On the basis of its properties of excellent brightness, high fluorescence quantum yield, low cost, and facile synthesis procedures in contrast to the organic dyes, we have proposed a label-free method for specific DNA detection based on SPEET process. It is a new assay utilizing the SPEET process between the fluorescent DNA/AgNC string and AuNP colloid. In the proposed SPEET-based method, the combination between visibility of color change of AuNP colloid and brighter fluorescence emission of DNA/AgNC string can supplement each other's advantages. This method shows a rapid response to the perfect-matched target with a good selectivity and in a concentration-dependent manner. Moreover, the label-free, enzyme-free, and thermal cycling-free strategy would be helpful to facilitate the development of a simple, low-cost, and portable detection system. Thus, we believe our findings would enable greater diversity of applications of DNA/AgNCs and open up new horizons for researchers to develop fluorescence turn-on biosensors

ASSOCIATED CONTENT

Supporting Information

Details about Figures S1−S9 and Table S1. The Supporting Information is available free of charge on the ACS Publications website at DOI: 10.1021/acsami.5b03837.

AUTHOR INFORMATION

Corresponding Authors
*E-mail: binchengyin@ecust.edu.cn.
*E-mail: bcye@ecust.edu.cn.
Notes
The authors declare no competing financial interest.

ACKNOWLEDGMENTS

REFERENCES

(1) Guo, S.; Wang, E. Noble Metal Nanomaterials: Controllable Synthesis and Application in Fuel Cells and Analytical Sensors. *Nano Today* **2011**, *6*, 240−264.
(2) Cobley, C. M.; Chen, J.; Cho, E. C.; Wang, L. V.; Xia, Y. Gold Nanostructures: a Class of Multifunctional Materials for Biomedical Applications. *Chem. Soc. Rev.* **2011**, *40*, 44−56.
(3) Xia, Y.; Xiong, Y.; Lim, B.; Skrabalak, S. E. Shape-Controlled Synthesis of Metal Nanocrystals: Simple Chemistry Meets Complex Physics. *Angew. Chem., Int. Ed.* **2009**, *48*, 60−103.
(4) Xu, H.; Suslick, K. S. Sonochemical Synthesis of Highly Fluorescent Ag Nanoclusters. *ACS Nano* **2010**, *4* (6), 3209−3214.
(5) Zheng, J.; Nicovich, P. R.; Dickson, R. M. Highly Fluorescent Noble-Metal Quantum Dots. *Annu. Rev. Phys. Chem.* **2007**, *58*, 409−431.
(6) Jin, R. Quantum Sized, Thiolate-Protected Gold Nanoclusters. *Nanoscale* **2010**, *2*, 343−362.
(7) Lin, C. A.; Lee, C. H.; Hsieh, J. T.; Wang, H. H.; Li, J. K.; Shen, J.L.; Chan, W. H.; Yeh, H. I.; Chang, W. H. Review: Synthesis of Fluorescent Metallic Nanoclusters toward Biomedical Application: Recent Progress and Present Challenges. *J. Med. Biol. Eng.* **2009**, *29*, 276−283.
(8) Braun, E.; Eichen, Y.; Sivan, U.; Ben-Yoseph, G. DNA-Templated Assembly and Electrode Attachment of a Conducting Silver Wire. *Nature* **1998**, *391*, 775−778.
(9) Guo, W.; Yuan, J.; Dong, Q.; Wang, E. Highly Sequence-Dependent Formation of Fluorescent Silver Nanoclusters in Hybridized DNA Duplexes for Single Nucleotide Mutation Identification. *J. Am. Chem. Soc.* **2010**, *132*, 932−934.
(10) Huang, Z.; Pu, F.; Hu, D.; Wang, C.; Ren, J.; Qu, X. Site-Specific DNA-Programmed Growth of Fluorescent and Functional Silver Nanoclusters. *Chemistry* **2011**, *17*, 3774−3780.
(11) Ma, K.; Cui, Q.; Liu, G.; Wu, F.; Xu, S.; Shao, Y. DNA Abasic Site-Directed Formation of Fluorescent Silver Nanoclusters for Selective Nucleobase Recognition. *Nanotechnology* **2011**, *22*, 305502.
(12) Li, J.; Zhong, X.; Cheng, F.; Zhang, J. R.; Jiang, L. P.; Zhu, J. J. One-Pot Synthesis of Aptamer-Functionalized Silver Nanoclusters for Cell-Type-Specific Imaging. *Anal. Chem.* **2012**, *84*, 4140−4146.
(13) Latorre, A.; Somoza, Á. DNA-Mediated Silver Nanoclusters: Synthesis, Properties and Applications. *Chem. Bio. Chem.* **2012**, *13*, 951−958.
(14) Gwinn, E. G.; O'Neill, P.; Guerrero, A. J.; Bouwmeester, D.; Fygenson, D. K. Sequence-Dependent Fluorescence of DNA-Hosted Silver Nanoclusters. *Adv. Mater.* **2008**, *20*, 279−283.

(15) Richards, C. I.; Hsiang, J. C.; Senapati, D.; Patel, S.; Yu, J. H.; Vosch, T.; Dickson, R. M. Optically Modulated Fluorophores for Selective Fluorescence Signal Recovery. *J. Am. Chem. Soc.* **2009**, *131*, 4619–4621.

(16) Sharma, J.; Yeh, H. C.; Yoo, H.; Werner, J. H.; Martinez, J. S. A Complementary Palette of Fluorescent Silver Nanoclusters. *Chem. Commun.* **2010**, *46*, 3280–3282.

(17) Su, Y. T.; Lan, G. Y.; Chen, W. Y.; Chang, H. T. Detection of Copper Ions through Recovery of the Fluorescence of DNA-Templated Copper/Silver Nanoclusters in the Presence of Mercapto-propionic Acid. *Anal. Chem.* **2010**, *82*, 8566–8572.

(18) MacLean, J. L.; Morishita, K.; Liu, J. DNA Stabilized Silver Nanoclusters for Ratiometric and Visual Detection of Hg$^{(2)(+)}$ and Its Immobilization in Hydrogels. *Biosens. Bioelectron.* **2013**, *48*, 82–86.

(19) Chen, J.; Zhang, X.; Cai, S.; Wu, D.; Chen, M.; Wang, S.; Zhang, J. A Fluorescent Aptasensor Based on DNA-Scaffolded Silver-Nanocluster for Ochratoxin A Detection. *Biosens. Bioelectron.* **2014**, *57*, 226–231.

(20) Liu, Y. Q.; Zhang, M.; Yin, B. C.; Ye, B. C. Attomolar Ultrasensitive MicroRNA Detection by DNA-Scaffolded Silver-Nanocluster Probe Based on Isothermal Amplification. *Anal. Chem.* **2012**, *84*, 5165–5169.

(21) Zhang, M.; Liu, Y. Q.; Yu, C. Y.; Yin, B. C.; Ye, B. C. Multiplexed Detection of Micrornas by Tuning DNA-Scaffolded Silver Nanoclusters. *Analyst* **2013**, *138*, 4812–4817.

(22) Yang, S. W.; Vosch, T. Rapid Detection of MicroRNA by a Silver Nanocluster DNA Probe. *Anal. Chem.* **2011**, *83*, 6935–6939.

(23) Shah, P.; Thulstrup, P. W.; Cho, S. K.; Bhang, Y. J.; Ahn, J. C.; Choi, S. W.; Bjerrum, M. J.; Yang, S. W. In-Solution Multiplex MiRNA Detection Using DNA-Templated Silver Nanocluster Probes. *Analyst* **2014**, *139*, 2158–2166.

(24) Yin, J.; He, X.; Wang, K.; Qing, Z.; Wu, X.; Shi, H.; Yang, X. One-Step Engineering of Silver Nanoclusters–Aptamer Assemblies as Luminescent Labels to Target Tumor Cells. *Nanoscale* **2011**, *4*, 110–112.

(25) Sharma, J.; Yeh, H. C.; Yoo, H.; Werner, J. H.; Martinez, J. S. Silver Nanocluster Aptamers: in Situ Generation of Intrinsically Fluorescent Recognition Ligands for Protein Detection. *Chem. Commun.* **2011**, *47*, 2294–2296.

(26) Li, T.; Zhang, L.; Ai, J.; Dong, S.; Wang, E. Ion-Tuned DNA/Ag Fluorescent Nanoclusters as Versatile Logic Device. *ACS Nano* **2011**, *5*, 6334–6338.

(27) Yeh, H. C.; Sharma, J.; Han, J. J.; Martinez, J. S.; Werner, J. H. A DNA-Silver Nanocluster Probe that Fluoresces upon Hybridization. *Nano Lett.* **2010**, *10*, 3106–3110.

(28) Zhang, M.; Guo, S. M.; Li, Y. R.; Zuo, P.; Ye, B. C. A Label-Free Fluorescent Molecular Beacon Based on DNA-Templated Silver Nanoclusters for Detection of Adenosine and Adenosine Deaminase. *Chem. Commun.* **2012**, *48*, 5488–5490.

(29) Yeh, H. C.; Sharma, J.; Shih, I.-M.; Vu, D. M.; Martinez, J. S.; Werner, J. H. A Fluorescence Light-Up Ag Nanocluster Probe that Discriminates Single-Nucleotide Variants by Emission Color. *J. Am. Chem. Soc.* **2012**, *134*, 11550–11558.

(30) Zhang, L. B.; Zhu, J. B.; Zhou, Z. X.; Guo, S. J.; Li, J.; Dong, S. J.; Wang, E. K. A New Approach to Light up DNA/Ag Nanocluster-Based Beacons for Bioanalysis. *Chem. Sci.* **2013**, *4*, 4004–4010.

(31) Li, J.; Zhong, X.; Zhang, H.; Le, X. C.; Zhu, J. J. Binding-Induced Fluorescence Turn-on Assay Using Aptamer-Functionalized Silver Nanocluster DNA Probes. *Anal. Chem.* **2012**, *84*, 5170–5174.

(32) Yin, J.; He, X.; Wang, K.; Xu, F.; Shangguan, J.; He, D.; Shi, H. Label-Free and Turn-on Aptamer Strategy for Cancer Cells Detection Based on a DNA-Silver Nanocluster Fluorescence upon Recognition-Induced Hybridization. *Anal. Chem.* **2013**, *85*, 12011–12019.

(33) Yin, B. C.; Ma, J. L.; Le, H. N.; Wang, S.; Xu, Z.; Ye, B. C. A New Mode to Light up an Adjacent DNA-Scaffolded Silver Probe Pair and Its Application for Specific DNA Detection. *Chem. Commun.* **2014**, *50*, 15991–15994.

(34) Dubertret, B.; Calame, M.; Libchaber, A. J. Single-Mismatch Detection Using Gold-Quenched Fluorescent Oligonucleotides. *Nat. Biotechnol.* **2001**, *19*, 365–370.

(35) Degliangeli, F.; Kshirsagar, P.; Brunetti, V.; Pompa, P. P.; Fiammengo, R. Absolute and Direct MicroRNA Quantification Using DNA-Gold Nanoparticle Probes. *J. Am. Chem. Soc.* **2014**, *136*, 2264–2267.

(36) Harry, S. R.; Hicks, D. J.; Amiri, K. I.; Wright, D. W. Hairpin DNA Coated Gold Nanoparticles as Intracellular mRNA Probes for the Detection of Tyrosinase Gene Expression in Melanoma Cells. *Chem. Commun.* **2010**, *46*, 5557–5559.

(37) Jayagopal, A.; Halfpenny, K. C.; Perez, J. W.; Wright, D. W. Hairpin DNA-Functionalized Gold Colloids for the Imaging of mRNA in Live Cells. *J. Am. Chem. Soc.* **2010**, *132*, 9789–9796.

(38) Song, S.; Liang, Z.; Zhang, J.; Wang, L.; Li, G.; Fan, C. Gold-Nanoparticle-Based Multicolor Nanobeacons for Sequence-Specific DNA Analysis. *Angew. Chem., Int. Ed.* **2009**, *48*, 8670–8674.

(39) Chen, C. W.; Wang, C. H.; Wei, C. M.; Hsieh, C. Y.; Chen, Y. T.; Chen, Y. F.; Lai, C. W.; Liu, C. L.; Hsieh, C. C.; Chou, P. T. Highly Sensitive Emission Sensor Based on Surface Plasmon Enhanced Energy Transfer between Gold Nanoclusters and Silver Nanoparticles. *J. Phys. Chem. C* **2009**, *114*, 799–802.

(40) Liu, J. M.; Chen, J. T.; Yan, X. P. Near Infrared Fluorescent Trypsin Stabilized Gold Nanoclusters as Surface Plasmon Enhanced Energy Transfer Biosensor and in Vivo Cancer Imaging Bioprobe. *Anal. Chem.* **2013**, *85*, 3238–3245.

(41) Yun, C. S.; Javier, A.; Jennings, T.; Fisher, M.; Hira, S.; Peterson, S.; Hopkins, B.; Reich, N. O.; Strouse, G. F. Nanometal Surface Energy Transfer in Optical Rulers, Breaking the FRET Barrier. *J. Am. Chem. Soc.* **2005**, *127*, 3115–3119.

(42) Grabar, K. C.; Freeman, R. G.; Hommer, M. B.; Natan, M. J. Preparation and Characterization of Au Colloid Monolayers. *Anal. Chem.* **1995**, *67*, 735–743.

(43) Ritchie, C. M.; Johnsen, K. R.; Kiser, J. R.; Antoku, Y.; Dickson, R. M.; Petty, J. T. Ag Nanocluster Formation Using a Cytosine Oligonucleotide Template. *J. Phys. Chem. C* **2007**, *111*, 175–181.

(44) Richards, C. I.; Choi, S.; Hsiang, J. C.; Antoku, Y.; Vosch, T.; Bongiorno, A.; Tzeng, Y. L.; Dickson, R. M. Oligonucleotide-Stabilized Ag Nanocluster Fluorophores. *J. Am. Chem. Soc.* **2008**, *130*, 5038–5039.

(45) Shukla, S.; Sastry, M. Probing Differential Ag$^+$–Nucleobase Interactions with Isothermal Titration Calorimetry (ITC): towards Patterned DNA Metallization. *Nanoscale* **2009**, *1*, 122–127.

(46) Chen, Y.; Yang, T.; Pan, H.; Yuan, Y.; Chen, L.; Liu, M.; Zhang, K.; Zhang, S.; Wu, P.; Xu, J. Photoemission Mechanism of Water-Soluble Silver Nanoclusters: Ligand-to-Metal–Metal Charge Transfer vs Strong Coupling between Surface Plasmon and Emitters. *J. Am. Chem. Soc.* **2014**, *136*, 1686–1689.

(47) Schultz, D.; Copp, S. M.; Markěsevic, N.; Gardner, K.; Oemrawsingh, S. S.; Bouwmeester, D.; Gwinn, E. Dual-Color Nanoscale Assemblies of Structurally Stable, Few-Atom Silver Clusters, as Reported by Fluorescence Resonance Energy Transfer. *ACS Nano* **2013**, *7*, 9798–9807.

(48) Shah, P.; Rørvig-Lund, A.; Chaabane, S. B.; Thulstrup, P. W.; Kjaergaard, H. G.; Fron, E.; Hofkens, J.; Yang, S. W.; Vosch, T. Design Aspects of Bright Red Emissive Silver Nanoclusters/DNA Probes for MicroRNA Detection. *ACS Nano* **2012**, *6*, 8803–8814.

(49) Li, H.; Rothberg, L. Colorimetric Detection of DNA Sequences Based on Electrostatic Interactions with Unmodified Gold Nano-particles. *Proc. Natl. Acad. Sci. U.S.A.* **2004**, *101*, 14036–14039.

(50) Zhang, Y.; Zhu, C.; Zhang, L.; Tan, C.; Yang, J.; Chen, B.; Wang, L.; Zhang, H. DNA-Templated Silver Nanoclusters for Multiplexed Fluorescent DNA Detection. *Small* **2015**, *11*, 1385–1389.